J Solid State Electrochem (2012) 16:2127–2133
DOI 10.1007/s10008-011-1627-x

ORIGINAL PAPER

Immobilization of DNA on a glassy carbon electrode based on Langmuir–Blodgett technique: application to the detection of epinephrine

Fei Wang · Ying Xu · Le Wang · Kui Lu · Baoxian Ye

Received: 29 August 2011 / Revised: 14 December 2011 / Accepted: 18 December 2011 / Published online: 4 January 2012

Abstract A double-stranded (ds) DNA-octadecylamine Langmuir–Blodgett film was attached to the surface of glassy carbon electrode (GCE) to create a novel voltammetric sensor (DNA-LB/GCE) for epinephrine (EP). Atomic force microscopy and electrochemical impedance spectroscopy were employed to study the characteristic of the DNA-LB film. The electrochemical behavior of EP at the modified electrode was investigated in pH 6.0 phosphate buffer solutions by cyclic voltammetry and amperometric methods. Compared with bare GCE, the DNA-LB/GCE sensor demonstrated an electrocatalytic effect on the oxidation of EP. In addition, the sensor shows excellent selectivity for EP detection, being free of interference from excess ascorbic acid and uric acid, and the method was also applied successfully to detect EP in the human urine samples.

Keywords Epinephrine · DNA · Octadecylamine · Langmuir–Blodgett film

Introduction

Epinephrine (EP) is one of the primary neurotransmitters in mammalian central nervous system [1, 2]. It controls the nervous system to perform a series of biological reactions and nervous chemical processes, and the changes of its concentration may result in many diseases [3]. Therefore, selective detection and measurement of EP levels are of great value and can aid in understanding the role of EP in the nervous system. The determination of EP is usually performed with high-performance liquid chromatography [4] and spectrophotometry [5–7]. Meanwhile, EP is an electroactive compound and can be determined by electrochemical methods [8–11]. However, the current electrochemical detection of EP has two challenges. One is its low concentration levels, and the irreversibility of its electrochemical property resulted in a large overpotential. Another challenge often encountered is the strong interference arising from electroactive ascorbic acid (AA) and uric acid (UA). To resolve these problems, one of the most common routes is using a modified electrode to improve the measuring sensitivity of EP and minimize the interference of AA and UA to EP determination [8–11]. Although many modified electrodes have been demonstrated to be effective for detecting EP, there is still a need to develop a new method with high efficiency and convenience for the detection of EP.

DNA-modified electrodes can be used as sensitive sensors for small molecules that interact with DNA [12–14], but one of the most important problems in electrochemical DNA sensors is the model immobilization of DNA onto electrode surfaces. Langmuir–Blodgett (LB) method is a convenient tool for designing artificial films with biological roles and has been applied to the fabrication of enzyme sensors [15], biomolecular microphotodiode [16], and biocatalysis membrane [17]. As far as we know, the report regarding immobilizing DNA by LB technique to design a voltammetric sensor is raised [18, 19] but very limited.

The previous work revealed a significant intercalation interaction between DNA and EP molecules [20] and demonstrated a DNA-modified electrode for selective determinations of EP [21]. In this approach, a new sensor has been

F. Wang · Y. Xu · L. Wang · B. Ye (✉)
Department of Chemistry, Zhengzhou University,
Zhengzhou 450052, People's Republic of China
e-mail: yebx@zzu.edu.cn

F. Wang · K. Lu
Department of Material and Chemistry Engineering,
Henan Institute of Engineering,
Zhengzhou 450007, People's Republic of China

developed based on DNA-LB film. To avoid DNA adsorption on the electrode surface before deposition, DNA-octadecylamine (DNA-ODA) LB film was formed by spreading DNA solution directly onto the subphase covered with a layer of ODA. The electrochemical behavior of EP at this modified electrode was investigated in detail. The experimental results showed that the DNA-modified electrode displayed an electrocatalytic response to EP. Moreover, the coexistence of AA and UA did not interfere with the determination of EP at this modified electrode, which makes the fabricated electrodes potential candidates for the detection of EP.

Experimental

Apparatus and reagents

EP and ODA were purchased from Sigma (Shanghai, China) and used without further purification. Fish sperm DNA was supplied by Shanghai Sangon Company (Shanghai, China) and used without pretreatment. ODA was dissolved in dichloromethane at a concentration of 1.0×10^{-3} mol L^{-1} to form a monolayer on the subphase. Stock solutions of 1 mg mL^{-1} DNA were prepared by dissolving an appropriate amount of the DNA in double-distilled water and were stored at 4 °C and used in not more than 5 days. All reagents were of analytical grade and were used as received.

CHI 650A electrochemical system (Shanghai, CHI Instrument Co. Ltd., China) and RST 5000 electrochemical analyzer (Shiruisi Instrument Technology Co. Ltd., Zhengzhou, China) were employed for electrochemical techniques. A standard three-electrode electrochemical cell was used for all electrochemical experiments with a bare GCE or modified electrode (d=3 mm) as working electrode, a platinum (Pt) wire as auxiliary electrode, and Ag/AgCl as reference electrode. LB films were performed with a JML-04 LB trough (Shanghai, Zhongchen Co. Ltd., China). The Langmuir trough, made of special non-porous PTFE, was 7×55 cm^2 in size.

Electrode pretreatment and DNA-modified procedure

The experiments were conducted at room temperature, at approximately 25 °C. Prior to deposition, the GCE was polished with finer emery paper and 0.1 μm alumina slurry and successively rinsed thoroughly with acetone, ethanol, and distilled water in ultrasonic bath for 1 min. Then, it was treated in 0.10 mol L^{-1} phosphate buffer (PB) solution (pH 5.0) by applying a potential of +1.75 V for 300 s under constant stirring. Finally, cyclic voltammetry (CV) was carried out in the same solution with a scan potential window between 0.30 and 1.25 V and with a scan rate of 50 mV s^{-1} until a stable CV profile was obtained [13].

ODA dichloromethane solutions were spread onto pure water using a micro-injector, allowing the solvent to evaporate for 30 min. Then, 400, 800, or 1,200 μL of DNA was spread carefully using a micro-injector onto the support aqueous subphase of the monolayer covered with a layer of ODA. Surface pressure was recorded immediately to evaluate the equilibrium between DNA and ODA monolayer interaction. When surface pressure reached quasi-equilibrium value at about 1 h, the pressure–area (π–A) isotherm was recorded using the JML-04 trough. The Langmuir film was compressed at a rate of 7 cm^2 min^{-1} and then transferred at a rate of 2.5 mm min^{-1} (vertical dipping) under the surface pressure of 35.0 mN m^{-1} onto GCE. This fabricated electrode was named DNA-LB/GCE. The multilayer films were assembled by sequential monolayer transfer. In the course of deposition, after each cycle of the upward and downward stroke, the GCE was kept dry completely in air for at least 1 h so that the following monolayer can be favorably transferred. For comparison, an ODA-modified electrode (without DNA) was fabricated by the same method, named ODA/GCE. Besides, 5 μL of 1 mg mL^{-1} DNA was cast on the GCE surface and dried. Then, a DNA film was formed. The conventional DNA-modified electrode was named DNA/GCE. Before use, the modified electrode was thoroughly rinsed with pure water and stored in 0.01 mol L^{-1} PB (pH=7.0) at 4 °C when not in use.

Results and discussion

π–A isotherms of DNA-LB films

Figure 1 shows surface pressure (π) versus area (A) isotherms of pure ODA film (curve a) and DNA-ODA film (curves b, c, d). The appreciable difference in the π–A

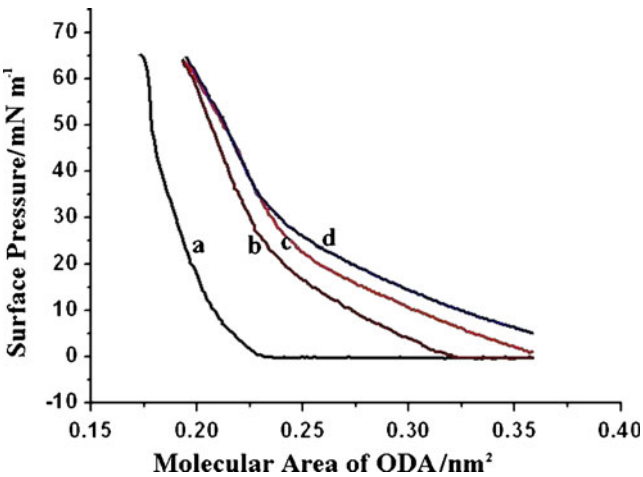

Fig. 1 π~A isotherms of ODA monolayer on pure water (curve a) and spreading different amounts of DNA onto subphase covered with a layer of ODA (*curves b*, *c*, *d*); *curve b*, 1.5 μg mL^{-1}; *curve c*, 3.0 μg mL^{-1}; *curve d*, 4.5 μg mL^{-1}

isotherms can be observed. From the π–A isotherm of pure ODA film, a steep rise curve in surface pressure was displayed during the compression process of the apparently condensed phase, and the limiting area of per molecule in condensed state was 0.22 nm^2 obtained by extrapolating the linear part of the isotherm to $\pi=0$, which are in agreement to those ones from the literature [15]. When DNA was spread carefully onto the subphase's interface covered with a layer of ODA, an increase of the initial surface pressure was observed. This is evidence that DNA molecules entered in ODA layer. At the same time, an expansion in the limiting molecular area value was shown, which was also evidence of ODA–DNA interaction, and the DNA molecules entered the ODA membrane at the air–water interface. Since the pH conditions are below the pK_a value of ODA, the major contribution to this interaction should be electrostatic interactions between the anionic phosphate groups of DNA and cationic R–NH_3^+. Besides, the isotherms for different amounts of DNA (the DNA contents were 1.5, 3.0, and 4.5 μg mL^{-1} for curves b, c, and d, respectively) are coincident with each other at high surface pressures, which meant that parts of DNA molecules were driven out during compressing process. The more DNA is added, the more the DNA molecules are expelled from mixed film. Thus, the same amount of DNA in ODA layer remains at high surface pressures.

To obtain a compact DNA-ODA LB film on electrode surface, the suitable amount of DNA was 3.0 μg mL^{-1} and the surface pressure of 35.0 mN m^{-1} was chosen to deposit the DNA-ODA LB film from air–water interface to electrode surface by vertical withdrawal method. The withdrawal speed was 2.5 mm min^{-1}.

Electrochemical impedance characterization of the DNA-LB/GCE

Figure 2 shows the Nyquist plots of electrochemical impedance spectroscopy (EIS) using bare GCE (curve a), ODA/GCE (curve b), and different layers of DNA-LB/GCE (curve c, d, e) in a solution of $K_3[Fe(CN)_6]/K_4[Fe(CN)_6]$ + 0.2 mol L^{-1} KCl, respectively. The whole of EIS has two parts: the linear segment at lower frequencies shows a controlled diffusion process; the semicircle part at higher frequencies corresponds to the electron transfer limited process or the electron transfer resistance (R_{ct}). It is easily seen that the R_{ct} of these electrodes was in the sequence: bare GCE <ODA/GCE <DNA-LB/GCE (Fig. 2, curves a–c), demonstrating that ODA or DNA-LB film was successfully modified on the GCE just as designed. This is because LB film acted as the blocking layer for electron and mass transfer that hinders further the diffusion of ferricyanide toward the electrode surface, and the negatively charged phosphate skeletons of DNA immobilized on the CILE had a repulsive force to $[Fe(CN)_6]^{3-/4-}$ anion, and therefore the R_{ct} at the DNA-LB/GCE decreased significantly. At the same time, an equivalent circuit as shown in the inset of Fig. 2 was designed, and the R_{ct} obtained was about 197, 336, and 513 Ω for one, two, and three layers of DNA-ODA LB film, respectively. Clearly, R_{ct} increased in linearity with the number of film layer, which suggests that the same amounts of DNA-ODA film increased with increasing the layers and immobilizing was uniform.

Atomic force microscopy of DNA-ODA LB films

Figure 3 shows typical atomic force microscopy (AFM) images of the silicon covered with one layer of DNA-ODA LB film under the surface pressure of 35.0 mN m^{-1}. The bare silicon showed even surface and had no impurity. However, it is clear that the AFM images of the silicon covered with one layer of DNA-ODA LB film showed aggregate structures of smaller round–oval spots and rope-like thing, which indicate that DNA have twined into the coiled structures and overlapped each other to form the aggregates in the composite films. Based on the results detailed above and the literature [22], we deduced the whole DNA-ODA LB film formation. Initially, some adsorbed DNA molecules under ODA monolayer serve as the seed nuclei. With the increased pressure, the nucleus density of DNA is high enough in the composite films, and then aggregates of compact clusters appeared.

Electrochemical behavior of EP at DNA-LB/GCE

Figure 4 displays the electrochemical responses of 2.0× 10^{-6} mol L^{-1} EP at bare GCE (curve a), ODA/GCE (curve b), DNA/GCE (curve c), and DNA-LB/GCE (curve d) in

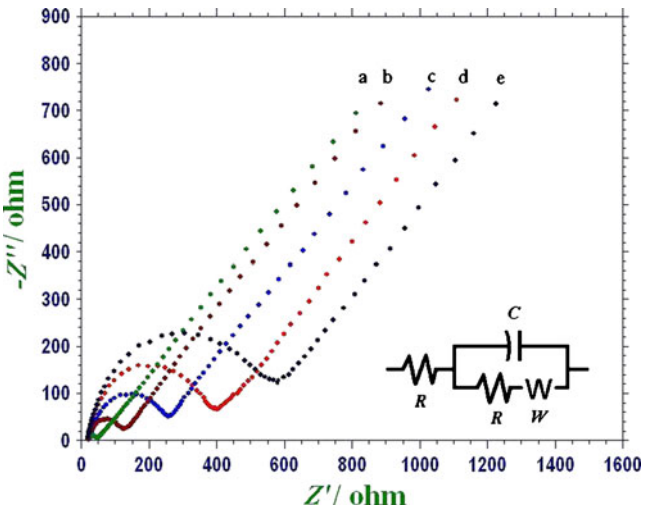

Fig. 2 Nyquist plots of bare GCE (*curve a*), ODA/GCE (*curve b*), and different layers DNA-LB/GCE (curves *c*, *d*, *e*) in 5× 10^{-3} mol L^{-1} $Fe(CN)_6^{3-/4-}$+0.2 mol L^{-1} KCl solution, respectively; *curve c*, one layer; *curve d*, two layers; *curve e*; three layers. The frequency range is from 1 MHz to 0.01 Hz, and the perturbation signal is 5 mV; the *inset* is equivalent circuit

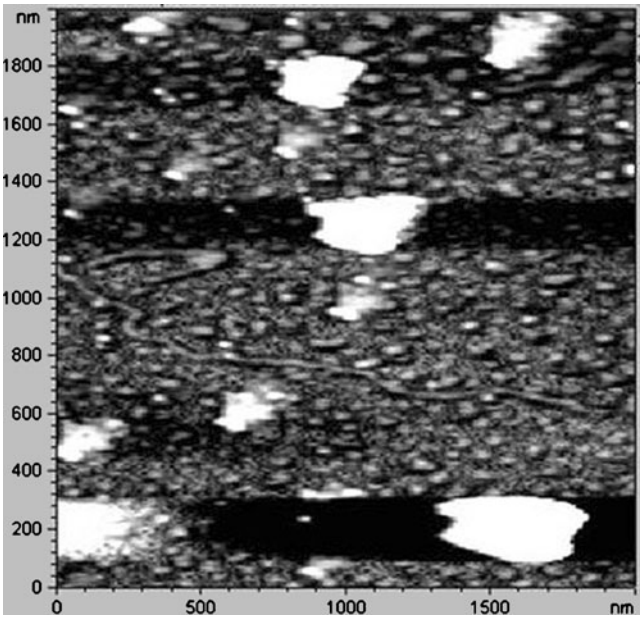

Fig. 3 AFM 2D topography images of the silicon covered with one layer of DNA-ODA LB film (scan area, 2×2 μm)

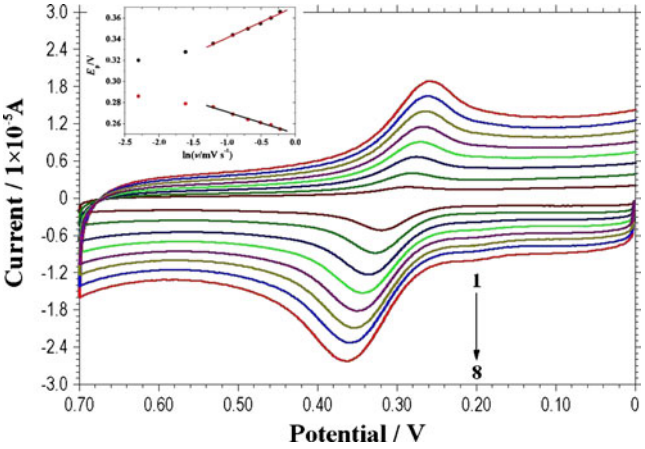

Fig. 5 Cyclic voltammograms of 2.0×10^{-6} mol L^{-1} EP at DNA-LB/GCE at different scan rates (from *1* to *8*, 0.10, 0.20, 0.30, 0.40, 0.50, 0.60, 0.70, 0.80 $V s^{-1}$); *insets* show the relationship of the peak potential E_{pa} against ln *v*; the other experimental conditions are the same as those described in Fig. 4

pH=6.0 PB solution, respectively. As can be seen, weak oxidation peaks could be discerned during the potential scan from 0.0 to 0.7 V, with no peak on the reverse scan, indicating the totally irreversible nature of the electrode reaction. In contrast, when DNA-LB/GCE was applied, a pair of well-defined redox appeared under the same experimental condition, of which the peak current is about tenfold, 3.8-fold, and 3.5-fold higher than that of bare GCE, ODA/GCE, and DNA/GCE oxidation peaks, respectively. The oxidation peak potential (E_{pa}) at the DNA-LB/GCE is the lowest. These results indicated that DNA-LB/GCE possessed a more excellent electrochemical response to EP. We calculate that the reasons for the notable sensitivity of the EP at the DNA-LB/GCE may be summarized as follows: (1) ds DNA layer have an enriched ability for EP due to an intercalative and electrostatic binding [23, 24] and (2) the aggregates of compact ds DNA layer greatly increase the electrode surface area, which could make EP easier to be accumulated and oxidized at a lower potential. To demonstrate these reasons, according to the equation [25], $i_{pa}=2.69\times10^{5}n^{3/2}Ac_0D^{1/2}v^{1/2}$, the area of DNA-LB/GCE is 0.071 cm^2, which is the biggest of all the electrodes. At the same time, according to Faraday's laws [26], $\Gamma^*=Q/(nFA)$, where *n* is the number of electron transferred, *F* is Faraday's constant, and *A* is the geometric surface area of the electrode; the average surface concentration of EP (Γ^*) was estimated to be 2.13×10^{-9} mol cm^{-2} at DNA-LB/GCE, which was about

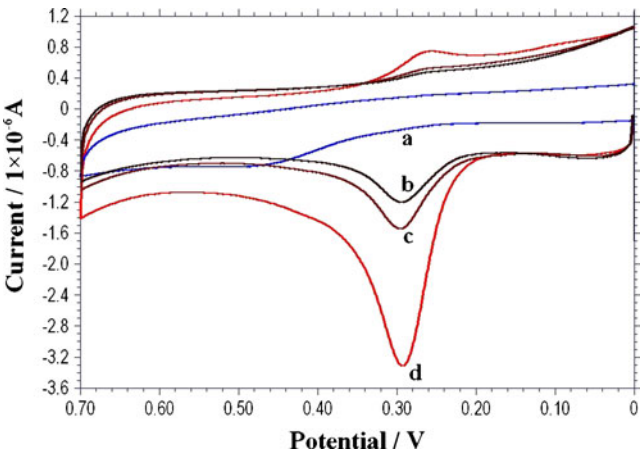

Fig. 4 Cyclic voltammograms of 2.0×10^{-6} mol L^{-1} EP at bare GCE (*curve a*), ODA/GCE (*curve b*), DNA/GCE (*curve c*), and DNA-LB/GCE (*curve d*) with scan rate v=0.05 $V s^{-1}$ in 0.2 mol L^{-1}, pH=6.0, phosphate-buffered solution

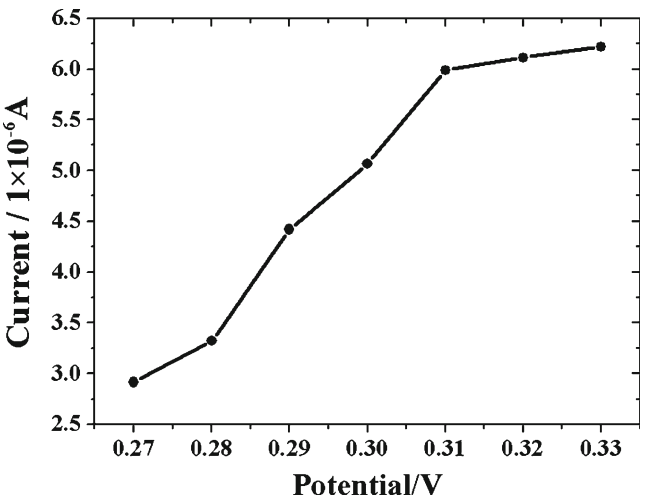

Fig. 6 Effect of the working potential on the DNA-LB/GCE response to 1.0×10^{-5} mol L^{-1} EP in 0.2 mol L^{-1} pH=6.0 phosphate-buffered solution

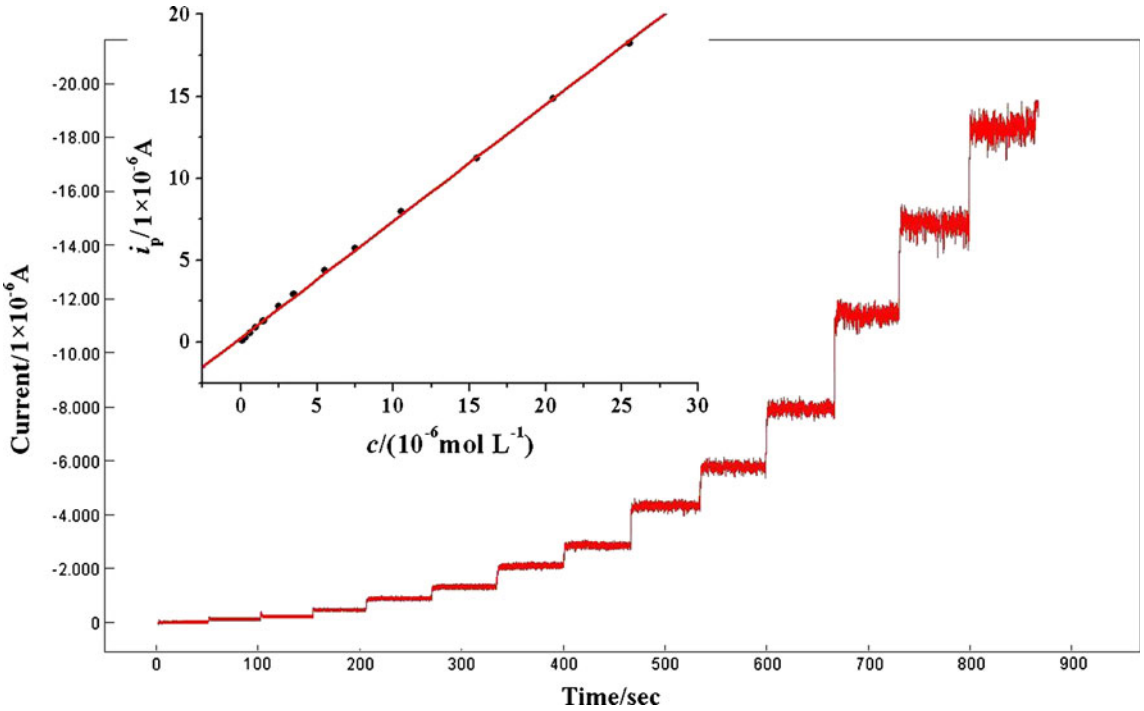

Fig. 7 Amperometric response of DNA-LB/GCE to the successive additions of EP at an applied potential of +0.31 V (vs Ag/AgCl); the *inset* is the calibration curve for EP

11.3, 4.1, and 5.2 times at the bare GCE, ODA/GCE, and DNA/GCE, respectively.

To further elucidate the electrode reaction of EP at the DNA-LB/GCE, the influence of potential scan rate (v) on i_p of 2.0×10^{-6} mol L^{-1} EP was studied by CV at different sweep rates from 100 to 1,000 mV s^{-1} (see Fig. 5). The redox peak currents of EP grow with the increase of scan rates and there are good linear relationships between i_p and v, indicating that the redox process of EP at the DNA-LB/GCE was adsorption-controlled. Meanwhile, the oxidation peak potentials shift positively and the reduction peak potentials shift negatively with the increasing scan rates, and good linear relationships are exhibited between peak potential (E_p) and ln$v$ (inset of Fig. 5). The two straight lines were derived from two linear regression equations as E_{pa} (V)=0.0264ln$v$+0.368 (γ=0.997) and E_{pc} (V)=−0.0238ln$v$+0.251 (γ=0.996). From the slope of E_{pa} vs. log(v), n=2 could be achieved, with the electron transfer coefficient α = 0.5 estimated from the peak width at half-height [27]. The results indicate that two electrons are involved in the oxidation of EP.

Analytical applications and methods validation

Optimization of experimental variables

The effect of solution pH on the response of EP was investigated by CV over the pH range of 5.0–8.0. Both the E_{pa} and E_{pc} shift negatively with the increase of solution pH, indicating that the electrocatalytic redox of EP at the DNA-LB/GCE is a proton-involved reaction. A linear regression equation was obtained as: $E^{0'}$ (V)=−0.068 pH+0.692 (γ=0.998). The slope is calculated to be

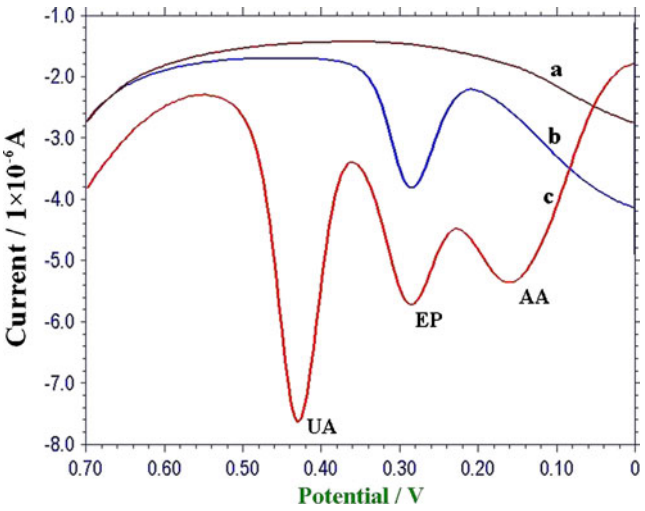

Fig. 8 Differential pulse anodic stripping voltammograms of blank solution (*curve a*), 2×10^{-6} mol L^{-1} EP (*curve b*), and 5×10^{-5} mol L^{-1} AA+2×10^{-6} mol L^{-1} EP+5×10^{-5} mol L^{-1} UA (*curve c*) at DNA-LB/GCE in 0.2 mol L^{-1} phosphate-buffered solution at pH 6.0

−68 mV pH^{-1} units over the studied pH range, which is very close to the theoretical value of −59 mV. It indicates that the electrocatalytic redox of EP at the DNA-LB-modified GCE is an equal-electron-and-proton process. Therefore, a mechanism for the EP redox may be expressed as follows:

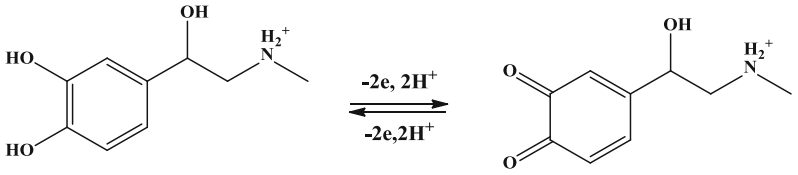

At the same time, the peak currents also change with pH and the largest anodic current appeared at pH 6.0. The effect of the applied potential on the steady-state current was also studied at the DNA-LB/GCE in pH 6.0 PB solution containing 1.0×10^{-5} mol L^{-1} EP (see Fig. 6). The steady-state current increases sharply when the applied potential shifts from 0.25 to 0.33 V and then reaches a plateau. At 0.31 V, sufficient current response was obtained; the background current was minimized, and interference from other electroactive species could be avoided or reduced. The applied potential of 0.31 V and pH 6.0 were thus selected for the amperometric determination of EP in subsequent experiments.

Amperometric response and calibration curve

Figure 7 presents the *i–t* curve resulting from the successive addition of different amounts of EP. A linear relationship between the oxidation currents and EP concentration was obtained from 5.0×10^{-7} to 5.0×10^{-5} mol L^{-1} (see inset in Fig. 7). The linear equation is presented as:

$$i_p(\mu A) = 0.250 + 0.712 \times 10^6 C$$

Here, a linear relative coefficient of 0.998 and a detection limit of 1.0×10^{-7} mol L^{-1} (S/N=3) were calculated.

Stability and reproducibility

The repeatability and stability of the DNA-LB/GCE was investigated by amperometric measurements of 1.0×10^{-5} mol L^{-1} EP. The relative standard deviation (RSD) for ten successive assays is 4.2%. When using five different electrodes, the RSD for five measurements is 5.1%. When stored in a pH 6.0 PB solution, the modified electrode retains 96% of its initial response after a week and 91% after 2 weeks. These results indicate that DNA-LB/GCE has good stability and reproducibility and could be used for EP measurements.

Interference study

It is well known that UA and AA coexist with EP in the extracellular fluid of the central nervous system and their concentration is much higher than that of EP. Hence, UA and AA are serious interfering substances for the electrochemical analysis of EP, and the interference from AA and UA was investigated. Figure 8 shows the differential pulse anodic stripping voltammograms of 5×10^{-5} mol L^{-1} AA+2×10^{-6} mol L^{-1} EP+5×10^{-5} mol L^{-1} UA in phosphate buffer (pH 6.0). Well-defined anodic peaks at 0.162, 0.285, and 0.430 mV for the oxidation of AA, EP and UA, respectively, were obtained at the DNA-LB/GCE. However, the presence of AA and UA does not modify significantly the signal for EP. However, dopamine is found to interfere with determination of EP under experimental conditions.

Determination of EP in a real sample

The release of catecholamines in the human system depends on smoking and exercise [28, 29]. Therefore, the proposed sensor has been examined for the determination of EP in the urine samples of a smoker and a nonsmoker. The samples were diluted with pH 6.0 PB solution before measurements were taken, and the results are shown in Table 1. The results indicate that the proposed method could be efficiently used for the determination of EP in the urine samples.

Table 1 Determination results of EP in the urine samples

Sample	Found[a] (1.0×10^{-6} mol L^{-1})	R.S.D	Added (1.0×10^{-6} mol L^{-1})	Found[a] (1.0×10^{-6} mol L^{-1})	Recovery (%)
Smoker's sample	0.64	3.2	4.00	4.79	103.8
Nonsmoker's sample	–[b]	–	4.00	4.26	106.5

[a]Average of three determination counts

[b]Below the detection limit

Conclusions

In summary, a novel DNA-LB/GCE is fabricated based on LB technique. The adsorptive voltammetric behaviors of EP at the DNA-LB/GCE were explored by means of CV. Compared with bare GCE, DNA-LB/GCE demonstrated a dramatic electrocatalytic effect on the oxidation of EP. In addition, the DNA-LB/GCE sensor shows excellent selectivity for EP detection, being free of interference from excess AA and UA. We believe that the DNA-LB/GCE fabricated here has provided an excellent starting point for developing a microelectrode, which has many potential uses.

Acknowledgements The authors gratefully acknowledge the financial support of National Natural Science Foundation of China (No. 20775073) and Natural Science Foundation of Henan Province in China (No. 2010B150007).

References

1. Banks WA (2001) Brain Res 899:209–217
2. Miranda-contreras L, Mendoza-Briceño RV, Palacios-Prü EL (1998) Int J Dev Neurosci 16:403–412
3. Schenk JO, Miller E, Adams RN (1983) J Chem Educ 60:311
4. Cooper BR, Mark Wightman R, Jorgenson JW (1994) J Chromatogr B-Bio Med Appl 653:25–34
5. Barnum DW (1977) Anal Chim Acta 89:157–166
6. Solich P, Polydorou CK, Koupparis MA, Efstathiou CE (2000) J Pharm Biomed Anal 22:781–789
7. James T (1973) J Pharm Sci 62:669–671
8. Wang L, Bai JY, Huang PF, Wang HJ, Zhang LY, Zhao YQ (2006) Electrochem Commun 8:1035–1040
9. Ni JA, Ju HX, Chen HY, Leech D (1999) Anal Chim Acta 378:151–157
10. Salimi A, Banks CE, Compton RG (2004) Analyst 129:225–228
11. Zhang HM, Zhou XL, Hui RT, Li NQ, Liu DP (2002) Talanta 56:1081–1088
12. Millan KM, Mikkelsen SR (1993) Anal Chem 65:2317–2323
13. Yang ZS, Zhao J, Zhang DP, Liu YC (2007) Anal Sci 23:569–572
14. Zhao J, Hu GZ, Yang ZS, Zhou YY (2007) Anal Lett 40:459–470
15. Yin F, Shin HK, Kwon YS (2005) Talanta 67:221–226
16. Caseli L, Zaniquelli MED, Furriel RPM, Leone FA (2002) Colloids Surf B 25:119–128
17. Oh SY, Park JK, Ko CB, Choi JW (2003) Biosens Bioelectron 19:103–108
18. Komarova E, Aldissi M, Bogomolova A (2005) Biosens Bioelectron 21:182–189
19. Wang F, Wu YJ, Liu JX, Ye BX (2009) Electrochim Acta 54:1408–1413
20. Zheng SJ, Lin XQ (2001) Chin Chem Lett 12:619–622
21. Jiang XH, Lin XQ (2005) Analyst 130:391–396
22. Dai SX, Zhang XT, Du ZL, Dang HX (2005) Mater Lett 59:423–429
23. Wang F, Wu YJ, Gao L, Xing TL, Ye BX (2009) Electroanalysis 21:1692–1698
24. Li J, Guo S, Zhai Y, Wang E (2009) Electrochem Commun 11:1085–1088
25. Faulkner LR (2001) Electrochemical method, fundamental and applications, 2nd edn. Wiley, New York
26. Bard AJ, Faulkner LR (1980) Electrochemical methods: fundamentals and applications. Wiley, New York
27. Laviron E (1979) J Electroanal Chem 101:19–28
28. Mendelson JH, Sholar MB, Goletiani N, Siegel AJ, Mello NK (2005) Neuropsychopharmacol 30:1751–1763
29. Tsuchida T, Fukuma N, Oikawa K, Kato K, Kato Y, Takano T, Kumita S (2007) J Nippon Med Sch 74:114–122